



Effect of supplementary cementing materials on concrete resistance against carbonation and chloride ingress

Vagelis G. Papadakis*

Danish Technological Institute, Building Technology Division, Concrete Centre, Taastrup, Denmark

Received 25 February 1999; accepted 3 December 1999

Abstract

In this work the durability of Portland cement systems incorporating supplementary cementing materials (SCM; silica fume, low- and high-calcium fly ash) is investigated. Experimental tests simulating the main deterioration mechanisms in reinforced concrete (carbonation and chloride penetration) were carried out. It was found that for all SCM tested, the carbonation depth decreases as aggregate replacement by SCM increases, and increases as cement replacement by SCM increases. The specimens incorporating an SCM, whether it substitutes aggregate or cement, when exposed to chlorides exhibit significantly lower total chloride content for all depths from the surface, apart from a thin layer near the external surface. New parameter values were estimated and existing mathematical models were modified to describe the carbonation propagation and the chloride penetration in concrete incorporating SCM. © 2000 Elsevier Science Ltd. All rights reserved.

Keywords: Carbonation; Chlorides; Fly ash; Modeling; Silica fume

1. Introduction

The majority of concrete deterioration cases is connected to corrosion of reinforcement due to carbonation- or chloride-induced depassivation of steel bars [1]. In urban and industrial areas, where environmental pollution results in a significant concentration of carbon dioxide, carbonation-initiated reinforcement corrosion prevails. Numerous surveys have indicated that chloride ions, originating from deicing salts or seawater, are the primary cause of reinforcing steel corrosion in highways and marine or coastal structures [2]. The chlorides that are transported through the concrete pore network and microcracks depassivate the oxide film covering the reinforcing steel and accelerate the reaction of corrosion. Even high-performance concrete may not necessarily ensure long-term durability in a severe environment unless it is designed for dimensional stability and soundness [3].

On the other hand, it has been well established [4] that sustainable development of the cement and concrete industries can be achieved by complete utilization of cementitious and pozzolanic by-products, such as fly ash, slag, and

silica fume, produced by thermal power plants and metallurgical industries. In addition to the effect on usual structural properties, such as strength and volume stability, the durability of concrete incorporating these supplementary cementing materials (SCM) should be taken into account. Despite the numerous contributions of a practical or experimental character regarding the effect of SCM on concrete durability [5–7], it is still not possible to identify the “ideal” concrete to provide optimum performance in a particular corrosive environment because of the numerous material, design, and environmental parameters involved in this problem [2]. In addition, efforts in the direction of a fundamental approach of SCM effect on concrete durability are very limited.

In previous publications [8,9], a simplified scheme describing the activity of silica fume and fly ash in terms of chemical reactions is proposed, yielding quantitative expressions for the estimation of the final chemical and volumetric composition of an SCM concrete.

In the present work, an experimental investigation of the effect of SCM (silica fume, low- and high-calcium fly ash) on Portland cement systems resistance against carbonation and chloride penetration was carried out, defining precisely what material is replaced when an SCM is added to the volume unit. Moreover, a theoretical approach to this effect is presented.

* Corresponding author. Titan Cement Company S.A., Kamari Plant, Department of Research & Development, P.O. Box 18, GR-192 00 Elefsis, Greece. Tel.: +30-1-553-7875; fax: +30-1-553-7790.

E-mail address: titanrdd@hol.gr (V.G. Papadakis)

2. Experimental program

2.1. Materials and mixture proportions

Three typical SCM (i.e., a silica fume, a low-calcium fly ash, and a high-calcium fly ash) were used, representing a wide range of chemical compositions, from highly pozzolanic to almost cementitious. The silica fume (SF) originated from Norway (Elkem Materials A/S, Kristiansand) and is a highly pozzolanic material. The low-Ca fly ash (FL) was produced in Denmark (Danasko I/S, Aalborg) and is categorized as normal pozzolanic material. The high-Ca fly ash (FH) was produced in Greece (Public Power Corporation, Ptolemais) and is a cementitious mineral admixture, which also has the most similar composition to a typical blast-furnace slag (GGBS) among all SCM tested. SF and FL were used as they were delivered from the producers, whereas FH was dry-pulverized prior to use to meet the FL mean particle size. A rapid-setting Portland cement was used (410 m²/kg Blaine's fineness). The physical and chemical characteristics of all materials are presented in Table 1. Normal graded sand and a common plasticizer (lignosulfonate) were used. Thus, only mortars were prepared; however, it is assumed that comparable conclusions derived from mortars may be also applicable to concrete.

A constant volume unit (1 m³) of mortar was chosen as a common basis. When an SCM was added to this unit, then an equal volume of another component, either cement or aggregate, was removed to keep the same total volume and the common comparison basis. The mixture proportions of mortar specimens prepared for the durability measurements are summarized in Table 2. In the control specimen the water-cement ratio (W/C) was 0.5 and the aggregate-cement ratio (A/C) was 3.

Table 1
Main physical, chemical, and mineralogical characteristics of cement, silica fume, and fly ashes

| | Cement | SF | FL | FH |
|--------------------------------------|--------|-------|-------|-------|
| Physical properties | | | | |
| Mean diameter (μm) | 14.0 | 0.36 | 13.9 | 12.6 |
| BET surface area (m ² /g) | 1.3 | 18 | 1.2 | 6.2 |
| Density (kg/m ³) | 3,130 | 2,260 | 2,250 | 2,660 |
| Chemical Analysis (%) | | | | |
| SiO ₂ | 20.10 | 90.90 | 53.50 | 39.21 |
| Al ₂ O ₃ | 4.25 | 1.12 | 20.40 | 16.22 |
| Fe ₂ O ₃ | 3.49 | 1.46 | 8.66 | 6.58 |
| CaO | 63.20 | 0.69 | 3.38 | 22.78 |
| Free CaO | 1.48 | 0.024 | 0.36 | 5.18 |
| MgO | 1.26 | 0.77 | 2.25 | 2.35 |
| Na ₂ O | 0.26 | 0.35 | 0.22 | 0.71 |
| K ₂ O | 0.34 | 0.57 | 0.52 | 1.22 |
| SO ₃ | 2.88 | 0.38 | 0.60 | 4.30 |
| Loss on ignition | 1.75 | 3.00 | 2.20 | 2.10 |
| Other characteristics | | | | |
| Insoluble residue (%) | 0.11 | 62.85 | 78.4 | 30.88 |
| Glass phase (%) | — | 96 | 75 | 50 |

In the case of aggregate replacement by SCM, three different amounts were selected according to SCM type: silica fume—5, 10, and 15% addition to cement mass (specimens SFA1, SFA2, and SFA3, respectively); low-Ca fly ash—10, 20, and 30% addition to cement mass (specimens FLA1, FLA2, and FLA3, respectively); and high-Ca fly ash—10, 20, and 30% addition to cement mass (specimens FHA1, FHA2, and FHA3, respectively).

In the case of cement replacement by SCM, the same amounts were also selected: silica fume—5, 10, and 15% replacement of the control cement mass (specimens SFC1, SFC2, and SFC3, respectively); low-Ca fly ash—10, 20, and 30% replacement of the control cement mass (specimens FLC1, FLC2, and FLC3, respectively); and high-Ca fly ash—10, 20, and 30% replacement of the control cement mass (specimens FHC1, FHC2, and FHC3, respectively).

The water content (kg/m³) was kept constant for all specimens.

The dry materials were mixed for 2 min. Then the water was added, containing the plasticizer (0.5% by weight of the cement plus SCM), and the mixing was continued for a further 2 min (representing standard practice). The mortar specimens were cast in steel cylinders of 100-mm diameter and 200-mm height, vibrated for 30 sec on a vibration table, and then hermetically sealed to minimize water evaporation. The molds were stripped after 24 h and the specimens were placed, separately for each mixture, underwater at 20°C [saturated in Ca(OH)₂], for 1 year. This long-term curing period underwater ensures an advanced degree of both Portland cement hydration and pozzolanic activity.

Table 2
Absolute and relative mixture proportions for mortar specimens^a

| Specimen | C | W | P | A | W/C | P/C | A/C |
|----------|-------|-------|-------|---------|-------|-------|------|
| Control | 514.6 | 257.4 | 0.0 | 1,543.8 | 0.50 | 0.00 | 3.00 |
| SFA1 | 514.6 | 257.4 | 25.7 | 1,513.4 | 0.50 | 0.05 | 2.94 |
| SFA2 | 514.6 | 257.4 | 51.5 | 1,483.0 | 0.50 | 0.10 | 2.88 |
| SFA3 | 514.6 | 257.4 | 77.2 | 1,452.6 | 0.50 | 0.15 | 2.82 |
| FLA1 | 514.6 | 257.4 | 51.5 | 1,482.7 | 0.50 | 0.10 | 2.88 |
| FLA2 | 514.6 | 257.4 | 102.9 | 1,421.7 | 0.50 | 0.20 | 2.76 |
| FLA3 | 514.6 | 257.4 | 154.4 | 1,360.6 | 0.50 | 0.30 | 2.64 |
| FHA1 | 514.6 | 257.4 | 51.5 | 1,492.1 | 0.50 | 0.10 | 2.90 |
| FHA2 | 514.6 | 257.4 | 102.9 | 1,440.5 | 0.50 | 0.20 | 2.80 |
| FHA3 | 514.6 | 257.4 | 154.4 | 1,388.8 | 0.50 | 0.30 | 2.70 |
| SFC1 | 488.8 | 257.4 | 25.7 | 1,535.3 | 0.527 | 0.053 | 3.14 |
| SFC2 | 463.1 | 257.4 | 51.5 | 1,526.9 | 0.556 | 0.111 | 3.30 |
| SFC3 | 437.4 | 257.4 | 77.2 | 1,518.4 | 0.588 | 0.176 | 3.47 |
| FLC1 | 463.1 | 257.4 | 51.5 | 1,526.6 | 0.556 | 0.111 | 3.30 |
| FLC2 | 411.7 | 257.4 | 102.9 | 1,509.4 | 0.625 | 0.250 | 3.67 |
| FLC3 | 360.2 | 257.4 | 154.4 | 1,492.3 | 0.715 | 0.429 | 4.14 |
| FHC1 | 463.1 | 257.4 | 51.5 | 1,536.0 | 0.556 | 0.111 | 3.32 |
| FHC2 | 411.7 | 257.4 | 102.9 | 1,528.3 | 0.625 | 0.250 | 3.71 |
| FHC3 | 360.2 | 257.4 | 154.4 | 1,520.5 | 0.715 | 0.429 | 4.22 |

^a C, W, P, A: kg of cement, water, supplementary cementing material (SF, FL or FH), and aggregate (sand), respectively, per m³ of total mortar volume (for zero air content); W/C, P/C, A/C: the water-cement, SCM-cement, and aggregate-cement ratio (by weight), respectively.

2.2. Accelerated carbonation experiments

Slices 90 mm thick were cut from the middle of the specimens and covered with a gas-tight paint on the cylindrical surface, leaving free the two opposite ends to be exposed to carbonation. Two samples for each mixture were taken. The test specimens were kept for 1 month in a laboratory environment to stabilize internal humidity. They were then placed in a chamber with a controlled 3% concentration of CO₂, temperature 25°C, and relative humidity 61% for 100 days (nordtest method NT Build 357, 1989). After carbonation, the specimens were cut normal to the exposed surfaces and the carbonation depth was determined by means of a phenolphthalein indicator. For each mixture, the average carbonation depth of the four measurements is reported.

2.3. Rapid chloride permeability tests

The AASHTO T277 rapid test method to rank the chloride penetration resistance of concrete by applying a potential of 60 V of direct current and measuring the charge passed through the specimen was followed. The tested mortar cores were slices 51 mm thick, cut from the middle of the initially 200-mm specimens and coated with watertight tape on their cylindrical surface.

2.4. Chloride penetration experiments

The remaining two slices, 70 mm thick, from the initial specimens were intended for long-term ponding experiments, according to nordtest method NT Build 443 (1995). Prior to immersion, the samples were coated with epoxy resin and then a 10-mm thick slice was removed from one end (the end closer to the middle of the initial specimen). The samples were immersed in a chloride solution (165 g NaCl/L) for 100 days. The temperature was kept constant at 20°C throughout the entire test period. At the end of the immersion period, the exposed surface was ground using a dry process to a diameter of 75 mm by removing thin successive layers from different depths (1–2, 3–4, 5–6, 8–10, 12–15, 18–21, and 21–24 mm from the external surface). The total chloride content of the powders was determined by the Volhard titration method in accordance with the method NT Build 208 (1984).

3. Carbonation results and modeling

3.1. Experimental results

The measured carbonation depths for all specimens are shown in Fig. 1 (mean variation about 10%). For all SCM tested, the carbonation depth decreases as aggregate replacement by SCM increases and increases as cement replacement by SCM increases. The frequently cited statement that as fly ash or SF reduce the amount of calcium hydroxide they may increase the carbonation rate is valid only for cement replacement. This is because not only the calcium hydroxide is carbonated, but also the calcium sili-

cate hydrate (CSH), which is the main product of pozzolanic reaction. Thus, for aggregate replacement by an SCM the total amount of carbonatable constituents remains almost the same and moreover the porosity decreases resulting in lower carbonation rates. For cement replacement by an SCM the total amount of carbonatable constituents decreases due to decrease in total CaO, resulting in higher carbonation rates. Drawing a comparison between results for 10% SCM addition either replacing aggregate or cement, the lowest carbonation depth is observed for high-Ca fly ash, then for low-Ca fly ash, and the highest for silica fume.

Despite the numerous controversial discussions in the literature about the effect of SCM on concrete carbonation, when experiments were designed as in the present paper, similar conclusions were drawn. For instance, when high amounts of fly ash replace part of the fine aggregates the carbonation depth decreases [10]. It has also been observed [11] in 5-year period of exposure in natural conditions that when fly ash or GGBS substitute cement the depth of carbonation increases. In addition, it has been found that concrete made with blended cements is subject to more rapid carbonation than normal Portland cement concrete [5,12].

3.2. Theoretical modeling

Let us suppose that 1 m³ of fresh concrete or mortar is composed as follows:

- C , kg cement/m³
- P , kg SCM (SF, FL, or FH)/m³
- A , kg aggregates/m³
- W , kg water/m³
- D , kg admixtures/m³
- ε_{air} , m³ of entrained or entrapped air/m³
- ρ_C , cement density (kg/m³)
- ρ_P , SCM density (kg/m³)
- ρ_A , aggregate density (kg/m³)
- ρ_W , water density (kg/m³)
- ρ_D , admixture density (kg/m³)

The following balance equation should be fulfilled [see Eq. (1)]:

$$C/\rho_C + P/\rho_P + A/\rho_A + W/\rho_W + D/\rho_D + \varepsilon_{\text{air}} = 1 \quad (1)$$

It has been shown [8,9] that in the case of “complete” hydration and pozzolanic action and for the present particular SCM the amounts of Ca(OH)₂ (CH), C₃S₂H₃ (CSH), in kg/m³ of concrete, and the total porosity of carbonated concrete, ε_c , are given as follows:

- for SF-Portland cement concrete (SF < 0.18 C):
 $\text{CH} = 0.29 C - 1.62 \text{ SF}$
 $\text{CSH} = 0.57 C + 2.49 \text{ SF}$
 $\varepsilon_c = (W - 0.267 C - 0.0278 \text{ SF})/1,000$
- for FL-Portland cement concrete (FL < 0.23 C):
 $\text{CH} = 0.30 C - 1.30 \text{ FL}$
 $\text{CSH} = 0.57 C + 1.25 \text{ FL}$
 $\varepsilon_c = (W - 0.268 C - 0.177 \text{ FL})/1,000$

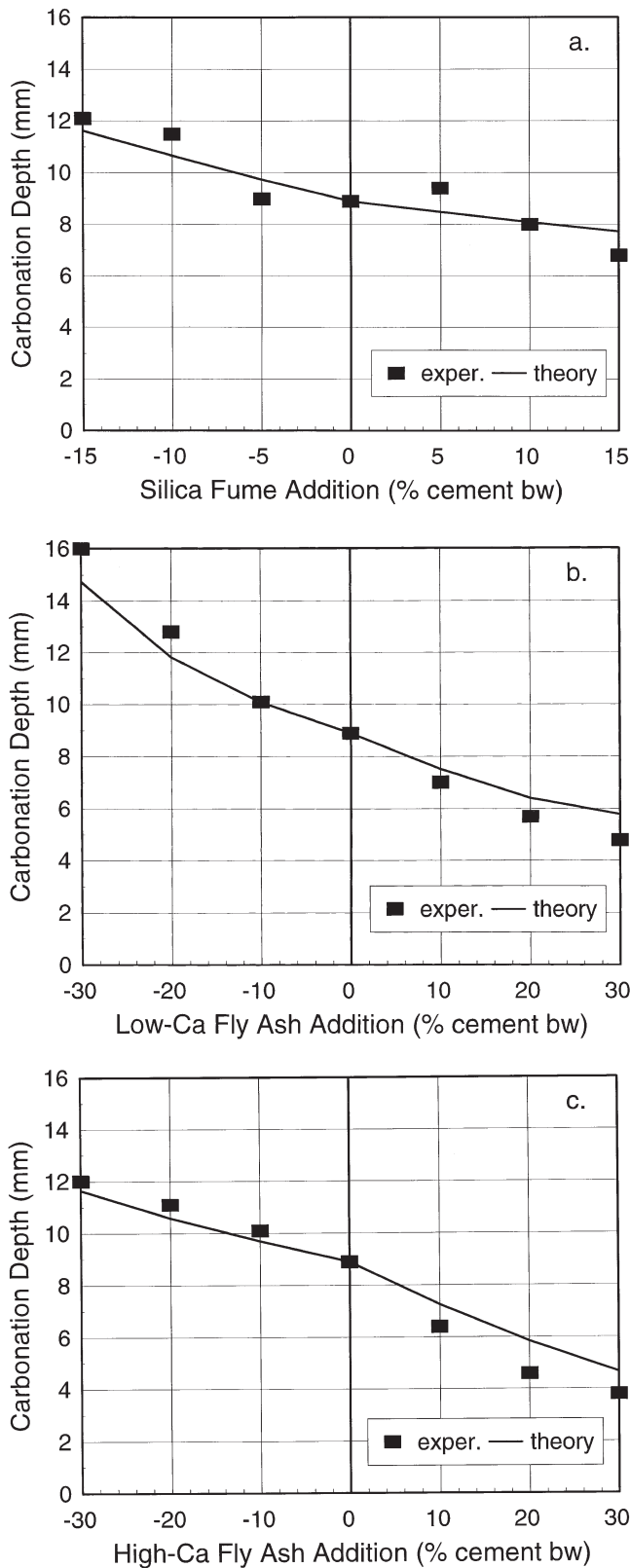


Fig. 1. Experimental results and model predictions of carbonation depth of mortars incorporating (a) silica fume, (b) low-calcium fly ash, and (c) high-calcium fly ash. The right-hand side refers to the case of aggregate replacement by SCM (constant water and cement content) and the left-hand side to the case of cement replacement by SCM (constant water and almost constant aggregate content).

- for FH-Portland cement concrete ($FH < 0.58 C$):
 $CH = 0.29 C - 0.50 FH$
 $CSH = 0.57 C + 0.79 FH$
 $\epsilon_c = (W - 0.267 C - 0.203 FH)/1,000$

The previous expressions may be used for the present mortars as they have been hydrated for a year and an advanced degree of reaction could be assumed.

Papadakis et al. [13,14] were the first to develop and experimentally verify a fundamental and comprehensive reaction engineering model of the processes leading to concrete carbonation. These processes include the diffusion of CO_2 in the gas phase of concrete pores, its dissolution in the aqueous film of these pores, the dissolution of solid $Ca(OH)_2$ in pore water, its ultimate reaction with the dissolved CO_2 , and the reaction of CO_2 with CSH and with some unhydrated phases of cement. The mathematical model yields a complex nonlinear system of differential equations in space and time and must be solved numerically for the unknown concentrations of the materials involved. For the usual range of parameters (especially, for relative humidity $> 50\%$), certain simplifying assumptions can be made that lead to the formation of a carbonation front, separating completely carbonated regions from those in which carbonation has not yet started. For one-dimensional geometry, the evolution of the carbonation depth x_c (m), with time t (s), is given by the analytical expression shown in Eq. (2):

$$x_c = \sqrt{\frac{2D_{e,CO_2}(CO_2/100)t}{0.33CH + 0.214CSH}} \quad (2)$$

where CO_2 is the CO_2 content in the ambient air at the concrete surface (%) and D_{e,CO_2} is the effective diffusivity of CO_2 in carbonated concrete (m^2/s). In an ambient relative humidity (RH), the diffusivity is given by the following empirical equation [15] [see Eq. (3)]:

$$D_{e,CO_2} = A \left(\frac{\epsilon_c}{\frac{C}{\rho_C} + \frac{P}{\rho_P} + \frac{W}{\rho_W}} \right)^a (1 - RH/100)^b \quad (3)$$

The parameters A , a , and b are $1.64 \cdot 10^{-6}$, 1.8, and 2.2, respectively, obtained from regression analysis of experimental data for $0.5 < W/C < 0.8$.

The intrinsic diffusion rate at which ions or molecules are transported in concrete depends on the size and connectivity of the pore system. As the W/C is lowered, the pore system becomes finer and less connected. Below $W/C = 0.45$, adequately cured concrete will develop a disconnected pore system, which will lead to very low transport rates [16]. Thus, the diffusion parameter values mentioned above are not valid for $W/C < 0.5$. Moreover, the SCM addition may further promote the pore disconnection. Using D_{e,CO_2} as an adjustable parameter and keeping the same exponent for the relative humidity term (i.e., 2.2), new parameter values were estimated so that the calculated carbonation depths from Eq. (2) agree with the experimental results. The opti-

imum parameter values are $6.1 \cdot 10^{-6}$ and 3 for A and a , respectively. These values are valid for $0.38 < W/(C + kP) < 0.58$, where k is the SCM efficiency factor for the 28-day compressive strength (2, 0.5, and 1 for SF, FL, and FH, respectively).

The predictions of Eq. (2) using the new parameters for the diffusivity are also shown in Fig. 1, and are in very good agreement with the corresponding experimental data.

4. Chloride penetration results and modeling

4.1. Rapid chloride permeability results

The rapid chloride permeability results for all specimens are presented in Fig. 2. The electrical charge passed through the control specimen may be higher than 4,000 Coulomb. This quite high value is due to high cement paste volume and the absence of coarse aggregate. All specimens incorporating an SCM, whether it substitutes aggregate or cement, exhibited lower electrical charge. Silica fume exhibited the lowest charge (10% SF, about 550 Coulomb), then low-calcium fly ash (10% FL, about 1,250 Coulomb), and high-calcium fly ash the highest (10% FH, about 3,000 Coulomb). The charge passed through a specimen was found inversely proportional to SCM content in mortar volume.

4.2. Normal chloride penetration results

The total chloride concentration profiles from the specimens immersed for 100 days in the chloride solution are shown in Fig. 3. As observed, the specimens incorporating an SCM, whether it substitutes aggregate or cement, exhibit significantly lower total chloride content for all depths from the surface, apart from a thin layer near the external mortar surface. However, when an SCM substitutes cement, the chloride content is higher than when it substitutes aggregate (although much lower than the control). Among all SCM tested, silica fume exhibited the lowest degree of chloride penetration, then low-calcium fly ash, and high-calcium fly ash exhibited the highest degree. As the SCM content in the mortar volume increases, the chloride content decreases.

In agreement with the above results, it has been found [11] that all mineral admixtures (fly ash, GGBS, silica fume) are efficient in preventing chloride ions from intruding into concretes under a marine environment for long-term tests.

4.3. Comparison between rapid and normal chloride penetration

A general qualitative agreement is observed between rapid (using an electrical field) and normal chloride penetration. However, it is observed from normal chloride penetration tests that when an SCM substitutes cement, the chloride content is higher than when it substitutes aggregate; this is not observed in rapid chloride penetration tests. The rapid tests are influenced from the interactions between ions and pore walls more than the normal tests. ASTM C1202 recog-

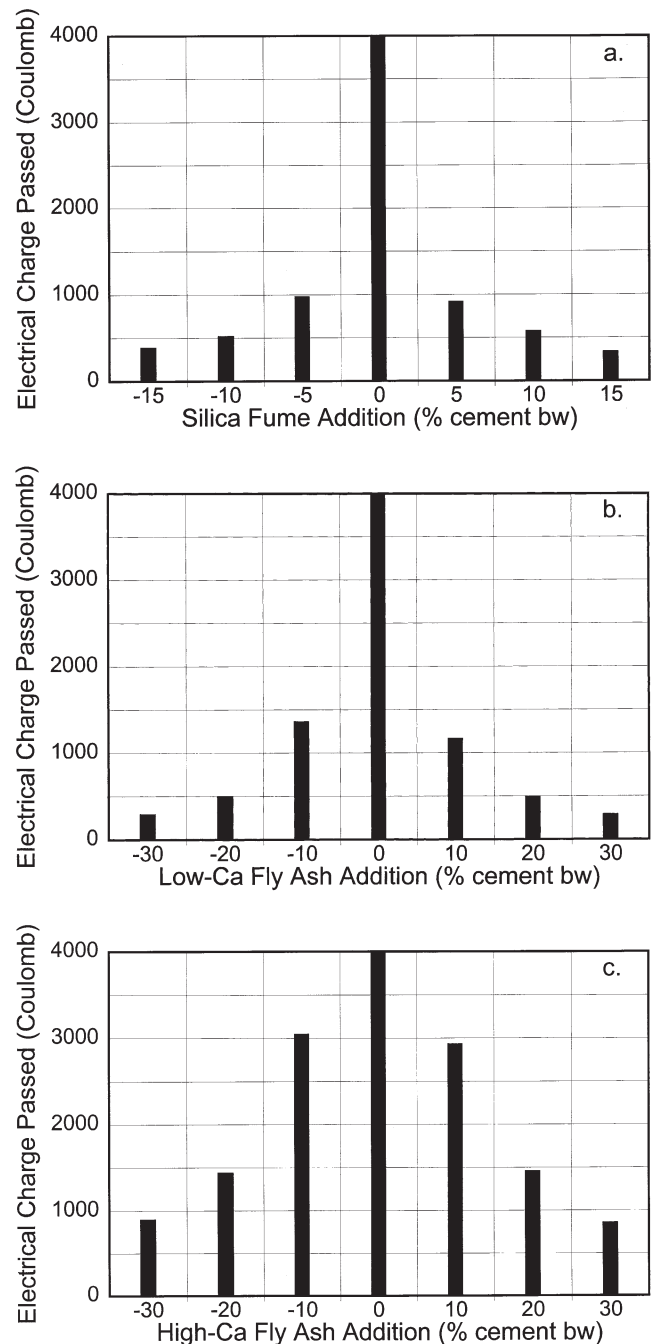


Fig. 2. Rapid chloride permeability of mortars incorporating (a) silica fume, (b) low-calcium fly ash, and (c) high-calcium fly ash. The right-hand side refers to the case of aggregate replacement by SCM and the left-hand side to the case of cement replacement by SCM.

nizes that a correlation between rapid chloride permeability test and long-period ponding test results should be established, while AASHTO T277 does not require this correlation.

As clearly indicated [17], it is not correct to use the passed charge from rapid tests to evaluate chloride permeability of concrete incorporating SCM. This is because the rapid test is a measurement of the electrical conductivity of

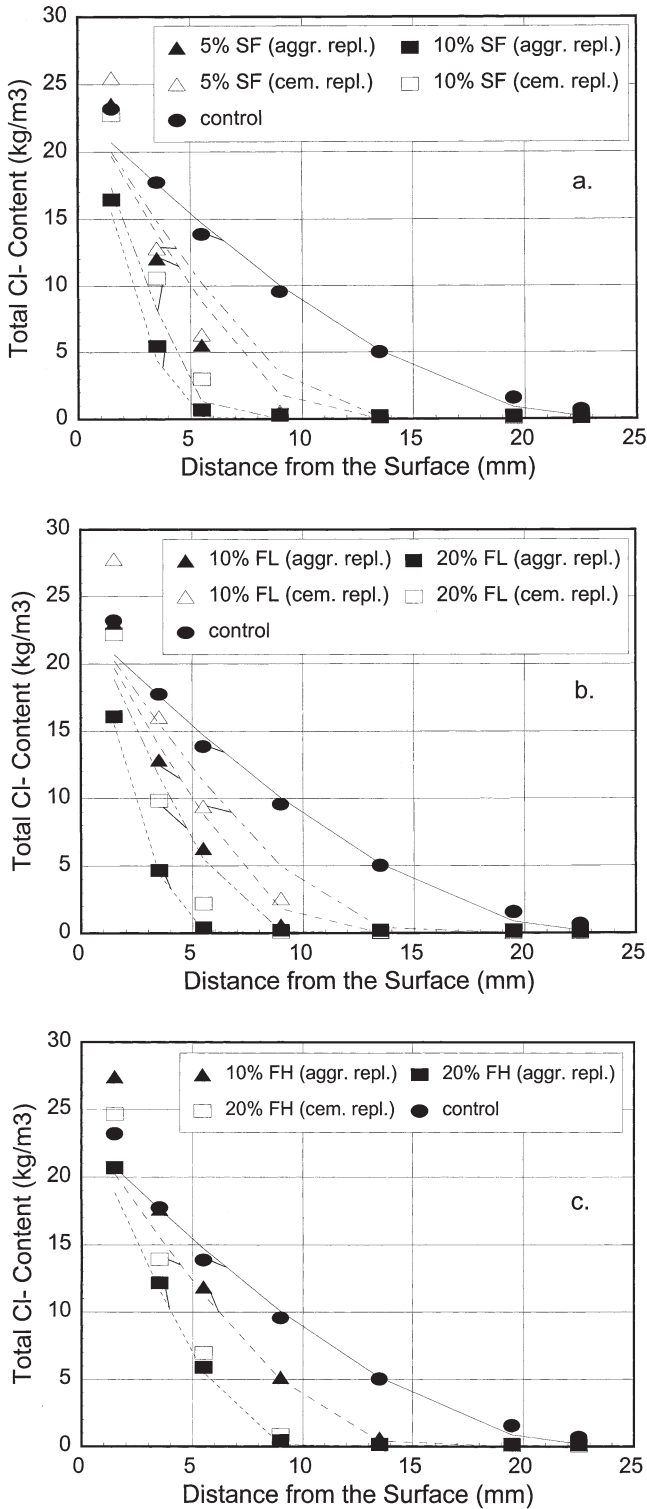


Fig. 3. Normal chloride penetration profiles for mortars incorporating (a) silica fume, (b) low-calcium fly ash, and (c) high-calcium fly ash (symbols: experimental data; lines: model predictions).

concrete, which depends on both pore structure and composition of the pore solution. The addition of SCM changes greatly the chemical composition of the pore solution, which has little to do with the pore structure itself.

4.4. Modeling of chloride diffusion and reaction in concrete

In many papers, chloride transport in concrete is modeled using Fick’s second law of diffusion, neglecting the chloride interaction with the solid phase. However, several field studies in recent years have indicated that the use of this law is not applicable to long-term chloride transport in concrete, very often calculating a decreasing chloride transport coefficient in time [18]. It is widely accepted that the transport behavior of chloride ions in concrete is a more complex and complicated process than can be described by Fick’s law of diffusion [19–21]. This approach, therefore, can be characterized as semiempirical, resulting in the calculation of an “apparent” effective diffusivity.

There is a generally good correlation between C_3A content (or C_4AF when there is lack of C_3A phase) and chloride binding capacity. There is also evidence for the binding of chlorides in CSH gel, possibly in interlayer space [22]. The Na^+ ions can be bound in CSH gel lattice [23], especially when the C/S ratio is low [6]. Several secondary chloride-calcium compounds have also been reported [24]. In addition to the chemical binding, the effects of ionic interaction, lagging motion of cations, and formation of an electrical double layer on the solid surface all play an important role in the transport of chloride ions in concrete [20]. The relationship between bound and free chlorides is nonlinear and may be expressed by the Langmuir equation [25], the Freundlich equation, or the modified Brunauer, Emmet and Teller (BET) equation [21]. Of these, the Langmuir equation is both fundamental and easier to use in practical applications.

Pereira and Hegedus [25] were the first to identify and model chloride diffusion and reaction in fully saturated concrete as a Langmuirian equilibrium process coupled with Fickian diffusion. Furthermore, Papadakis et al. [26,27] generalized this pioneering model effort of Pereira and Hegedus and extended it to more general conditions, offering an alternative simpler, yet equally accurate, numerical and analytical solution. By introducing a chloride-solid phase interaction term, the calculation of an “intrinsic” effective diffusivity is possible.

The physicochemical processes of diffusion of Cl^- in the aqueous phase of pores, their adsorption and binding in the solid phase of concrete, and their desorption are described by a nonlinear partial differential equation for the concentration of Cl^- in the aqueous phase $[Cl^-(aq)]$ (kg/m^3 pore solution), from which that of Cl^- bound in the solid phase $[Cl^-(s)]$ (kg/m^3 concrete) can be computed algebraically [26], as seen in Eqs. (4) and (5):

$$\frac{\partial [Cl^-(aq)]}{\partial t} = \frac{D_{e,Cl^-} \{1 + K_{eq}[Cl^-(aq)]\}^2}{K_{eq}[Cl^-(s)]_{sat} + \epsilon \{1 + K_{eq}[Cl^-(aq)]\}^2} \frac{\partial^2 [Cl^-(aq)]}{\partial x^2} \quad (4)$$

$$[\text{Cl}^-(s)] = \frac{K_{eq}[\text{Cl}^-(aq)]}{1 + K_{eq}[\text{Cl}^-(aq)]} [\text{Cl}^-(s)]_{\text{sat}} \quad (5)$$

initial condition: $[\text{Cl}^-(aq)] = [\text{Cl}^-(aq)]_{in}$ at $t = 0$ (initial concentration);

boundary conditions: $[\text{Cl}^-(aq)] = [\text{Cl}^-(aq)]_0$ at $x = 0$ (concrete surface) and $\partial[\text{Cl}^-(aq)]/\partial x = 0$ at $x = M$ (axis of symmetry)

In these equations, x is the distance from the concrete surface (m); t is the time (s); $D_{e,\text{Cl}}$ denotes the intrinsic effective diffusivity of Cl^- in concrete (m^2/s); K_{eq} is the equilibrium constant for Cl^- binding (m^3 of pore solution/kg); $[\text{Cl}^-(s)]_{\text{sat}}$ is the saturation concentration of Cl^- in the solid phase (kg/m^3 concrete); and ε is the concrete porosity (m^3 pore volume/ m^3 concrete). As observed from Eq. (5), the chloride binding capacity depends both on $[\text{Cl}^-(s)]_{\text{sat}}$ (content of sites that can bind chlorides) and K_{eq} (ratio of adsorption to desorption rate constants).

Eq. (4) can be solved only numerically. The solution allows estimation of the time required for the chloride concentration surrounding the reinforcement to increase over the threshold of depassivation of reinforcing bars.

As observed from Eq. (4), chloride ingress is retarded as $D_{e,\text{Cl}}$ decreases, $[\text{Cl}^-(s)]_{\text{sat}}$ increases, or K_{eq} increases. When an SCM is added in concrete, chloride binding capacity increases, as the present experimental results showed (higher total chloride content in a thin layer near the external mortar surface). This may be attributed to higher CSH content, especially that with lower C/S ratio, which can bind Na^+ ions and, therefore, the accompanying Cl^- . On the other hand, the pore restructuring due to pozzolanic products may decrease intrinsic diffusivity as well. In Fig. 4 a scanning electron micrograph of 10% silica fume-cement paste after 14 days of hydration is shown. As observed, a fine network of pozzolanic product (CSH) has been created in the middle of a capillary pore, acting as a trap for chlorides. Using atomic force microscopy [28], it was found that the internal surface of the SCM cement pastes presents small spheroid bulges giving an additional roughness.

The picture is different when a noninteracting molecule diffuses in a concrete incorporating SCM, as observed from the carbonation results of the present work. The ratio of oxygen to chloride diffusion coefficients was found constant for OPC pastes of high W/C ratio, but can attain high values for fine-textured blended cement pastes that have not suffered drying/carbonation [29]. It has also been reported [30] that this ratio increases as W/C ratio decreases. Also, it was found [31] that in the presence of chlorides the diffusivity of dissolved oxygen into saturated concretes decreases over and above the decrease of oxygen solubility in solution. It has also been reported [32] that up to a fly ash level of 33% the intrinsic air permeability remains fairly constant and then is higher compared to the control. The apparent chloride diffusion coefficient was found to decrease by a factor of 7. Chloride binding capacity increases by a factor of four

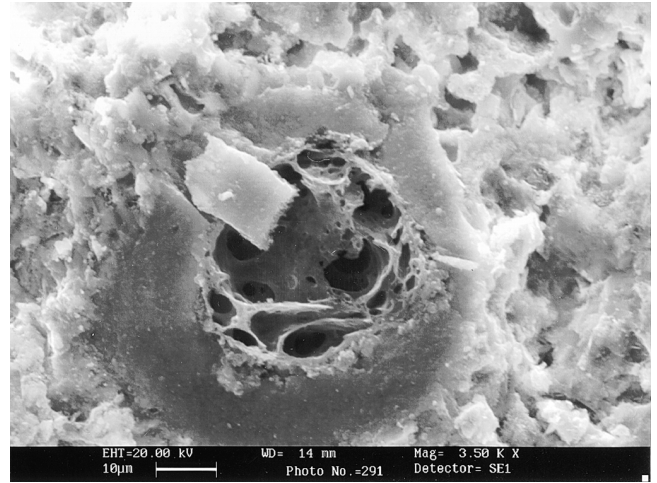


Fig. 4. Scanning electron micrograph (3,500 \times) of 10% silica fume-cement paste after 14 days of hydration.

and then remains constant. It seems, therefore, that chloride binding capacity is the determining factor in improving resistance to chloride ingress.

4.4.1. Parameter estimation

In the case of “complete” hydration and pozzolanic action, the total porosity of concrete can be calculated using the mathematical expressions given elsewhere [8,9]. However, for the oxide analyses of the present SCM, these expressions are simplified as follows:

- for SF-Portland cement concrete (SF < 0.18 C):
 $\varepsilon = \varepsilon_{\text{air}} + (W - 0.226 C)/1,000$
- for FL-Portland cement concrete (FL < 0.23 C):
 $\varepsilon = \varepsilon_{\text{air}} + (W - 0.227 C - 0.188 \text{FL})/1,000$
- for FH-Portland cement concrete (FH < 0.58 C):
 $\varepsilon = \varepsilon_{\text{air}} + (W - 0.226 C - 0.193 \text{FH})/1,000$

The intrinsic effective diffusivity of Cl^- in concrete (m^2/s) can be estimated by the following semiempirical equation [27 (for NaCl); see Eq. (6)]:

$$D_{e,\text{Cl}^-} = \frac{2.4 \cdot 10^{-10}}{\left(\frac{C + kP}{\rho_c} + \frac{W}{\rho_w}\right)^2} (\varepsilon_{\text{eff}})^n \quad (6)$$

Parameter $n = 3$ for $0.5 < W/C < 0.7$ and $0 < A/C < 6$; for CaCl_2 the numerator is 2×10^{-10} ; where k is the efficiency factor of the SCM for chloride penetration, P is the content of SF, FL, or FH in concrete (kg/m^3), and ε_{eff} is an effective, for diffusion, porosity, calculated as shown in Eq. (7):

$$\varepsilon_{\text{eff}} = W/\rho_w - 0.226 \cdot 10^{-3} (C + kP) \quad (7)$$

In seawater attack, the chloride concentration in the aqueous solution at the concrete surface, $[\text{Cl}^-(aq)]_0$ (kg/m^3 pore solution), depends on the sea (e.g., Atlantic ocean: 20 kg/m^3 , North Sea: 16 kg/m^3 , and Baltic Sea: 4 kg/m^3). In the case of deicing salts, the precise estimation of $[\text{Cl}^-(aq)]_0$ is difficult due to many involved parameters (frequency and

quantity of salt spreading, amount of available water from rain or melted snow for salt dissolution, etc.).

Parameters $[Cl^-(s)]_{sat}$ and K_{eq} can be determined from chloride binding isotherms. An experimental approach described elsewhere [32] was followed. The equilibrium constant for Cl^- binding was found fairly constant for all mixtures ($K_{eq} = 0.1 \text{ m}^3$ of pore volume/kg Cl^-). For the saturation concentration of Cl^- in the solid phase, the following empirical expression may be used, which is in good agreement with previously reported results [e.g., 21,27; see Eq. (8)]:

$$[Cl^-(s)]_{sat} = 8.8 \cdot 10^{-3}(C + kP) \quad (8)$$

4.4.2. Model predictions and comparison with the experimental data

Eq. (4) was solved numerically using a finite difference method. A Windows-based program, developed in Danish Technological Institute, was used. The total specimen length ($M = 0.06 \text{ m}$) was divided into 60 equal cells and a time step of 60 s was used. The Cl^- concentration in the solution at the specimen surface was $94.82 \text{ kg } Cl^-/\text{m}^3$. In order for the model predictions to fit the experimental data for the control specimen, an optimum value of parameter n in Eq. (6) of 3.5 was estimated. This is due to the significant decrease in pore connectivity for $W/C < 0.5$, as also described in carbonation modeling.

In Fig. 3, the model predictions (i.e., applying the Eqs. (4) through (8) for the total Cl^- concentration, $\epsilon[Cl^-(aq)] + [Cl^-(s)]$, as a function of the distance from the outer concrete surface, are presented. For these predictions to fit the experimental data, the following optimum efficiency factors were estimated:

- $k = 6$ for silica fume,
- $k = 3$ for low-calcium fly ash,
- $k = 2$ for high-calcium fly ash.

Good general agreement between model predictions using the above k values and experimental data is observed. These significantly higher k values for SCM efficiency against chlorides, compared with the corresponding values for strength (2, 0.5, and 1 for SF, FL, and FH, respectively) can be explained as due to important interactions of Cl^- with the pore walls, or by the electrical double layer at the pore walls-pore solution interface. Another important observation is that k values depend proportionally on the silica content of SCM (and therefore, on CSH content), as also observed in the case of strength [8,9].

5. Conclusions

1. It was established that for all supplementary cementing materials tested (silica fume, low- and high-calcium fly ash), the carbonation depth decreases as aggregate replacement by SCM increases, and increases as cement replacement by SCM increases. The lowest carbonation depth is observed for high-Ca fly ash, then for low-Ca fly ash, and the highest for silica fume. New parameter values were estimated and used

in an existing mathematical model to describe the carbonation of concrete incorporating SCM.

2. The specimens incorporating an SCM, whether it substitutes aggregate or cement, exhibit significantly lower total chloride content for all depths from the surface, apart from a thin layer near the external surface. Of all SCM tested, silica fume exhibited the lowest degree of chloride penetration, then low-calcium fly ash, and high-calcium fly ash the highest. High efficiency factors for resistance against chloride penetration of 6, 3, and 2 for silica fume, low-Ca fly ash, and high-Ca fly ash, respectively, were estimated (where Portland cement has by definition an efficiency factor equal to 1) and used in a modified mathematical model to describe the chloride penetration in concrete incorporating SCM.
3. A general qualitative agreement is observed between rapid (using an electrical field) and normal chloride penetration. A correlation between rapid chloride permeability test and long-period ponding test results should be established for quantitative conclusions.
4. The use of silica fume or fly ash has a significantly higher effect on the chloride transport than on a similarly sized neutral gas molecule because of the interactions with the charged pore walls, or by the electrical double layer at the pore walls-pore solution interface.
5. The use of SCM as an addition to a concrete mix, replacing either aggregates or cement, significantly lengthens the chloride-induced corrosion initiation stage. The use of SCM as an addition to a concrete mix, replacing aggregates, also lengthens the carbonation-induced corrosion initiation stage. However, the use of SCM as a cement replacement may result in a shortened carbonation-induced initiation stage and thereby increase the risk of corrosion.

Acknowledgments

The European Commission (DG XII- Training & Mobility of Researchers Programme) and the Danish Technological Institute (DTI—Building Technology Division, Concrete Centre) provided financial support for this work. The assistance of Mr. E.J. Pedersen (DTI) and the DTI-Concrete Centre staff is gratefully acknowledged.

References

- [1] P.A.M. Basheer, S.E. Chidiac, A.E. Long, Predictive models for deterioration of concrete structures, *Constr Build Mater* 10 (1996) 27–37.
- [2] N.G. Thompson, D.R. Lankard, Improved concretes for corrosion resistance, Georgetown Pike, McLean VA, US Department of Transportation, Federal Highway Administration, Report No. FHWA-RD-96-207, 1997.
- [3] P.K. Mehta, Durability—Critical issues for the future, *Concr Intern* 19 (1997) 27–33.
- [4] P.K. Mehta, Role of pozzolanic and cementitious material in sustain-

- able development of the concrete industry, in: Proceedings of the 6th International Conference on the Use of Fly Ash, Silica Fume, Slag, and Natural Pozzolans in Concrete, ACI SP-178, 1–25, Bangkok, 1998.
- [5] E.E. Berry, V.M. Malhotra, Fly ash in concrete, in: V.M. Malhotra (Ed.), *Supplementary Cementing Materials for Concrete*, Ottawa, CANMET SP-86-8E, 1987, 35–163.
- [6] E.J. Sellevold, T. Nilsen, Condensed silica fume in concrete: A world review, in: V.M. Malhotra (Ed.), *Supplementary Cementing Materials for Concrete*, Ottawa, CANMET SP-86-8E, 1987, 165–243.
- [7] A.M. Neville, *Properties of Concrete*, Longman, Essex, 1995.
- [8] V.G. Papadakis, Experimental investigation and theoretical modeling of silica fume activity in concrete, *Cem Concr Res* 29 (1999) 79–86.
- [9] V.G. Papadakis, Effect of fly ash on Portland cement systems. Part I: Low-calcium fly ash, *Cem Concr Res* (11) (1999) 1727–1736.
- [10] K.R. Hwang, T. Noguchi, F. Tomosawa, Effects of fine aggregate replacement on the rheology, compressive strength and carbonation properties of fly ash and mortar, in: Proceedings of the 6th International Conference on the Use of Fly Ash, Silica Fume, Slag, and Natural Pozzolans in Concrete, ACI SP-178, 401–410, Bangkok, 1998.
- [11] T. Sasatani, K. Torii, M. Kawamura, Five-year exposure test on long-term properties of concretes containing fly ash, blast-furnace slag, and silica fume, in: Proceedings of the 5th International Conference on the Use of Fly Ash, Silica Fume, Slag and Natural Pozzolans in Concrete, ACI SP-153, 283–296, Milwaukee, 1995.
- [12] V.G. Papadakis, M.N. Fardis, C.G. Vayenas, Hydration and carbonation of pozzolanic cements, *ACI Mater J* 89 (1992) 119–130.
- [13] V.G. Papadakis, C.G. Vayenas, M.N. Fardis, Fundamental modeling and experimental investigation of concrete carbonation, *ACI Mater J* 88 (1991) 363–373.
- [14] V.G. Papadakis, M.N. Fardis, C.G. Vayenas, Effect of composition, environmental factors and cement-lime mortar coating on concrete carbonation, *Mater and Struct* 25 (1992) 293–304.
- [15] V.G. Papadakis, C.G. Vayenas, M.N. Fardis, Physical and chemical characteristics affecting the durability of concrete, *ACI Mater J* 88 (1991) 186–196.
- [16] F. Young, Sulfate attack, *Concr Intern* 20 (1998) 7 (p. 7).
- [17] C. Shi, J.A. Stegemann, R.J. Caldwell, Effect of supplementary cementing materials on the specific conductivity of pore solution and its implications on the rapid chloride permeability test (AASHTO T277 and ASTM C1202) results, *ACI Mater J* 95 (1998) 389–394.
- [18] P. Sandberg, K. Petterson, O. Jørgensen, Field studies of chloride transport into high-performance concrete, in: Proceedings of the 3rd CANMET/ACI International Conference on Concrete in Marine Environment, ACI SP-163, 233–254, St. Andrews by-the-Sea, 1996.
- [19] M.H. Decter, N.R. Short, C.L. Page, D.D. Higgins, Chloride ion penetration into blended cement pastes and concrete, in: Proceedings of the 3rd International Conference on the Use of Fly Ash, Silica Fume, Slag and Natural Pozzolans in Concrete, ACI SP-114, 1399–1410, Trondheim, 1989.
- [20] T. Zhang, O.E. GjØrv, Diffusion behavior of chloride ions in concrete, *Cem Concr Res* 26 (1996) 907–917.
- [21] L. Tang, Chloride transport in concrete—Measurement and prediction, Chalmers University of Technology, Department of Building Materials, Gothenburg, Publication P-96:6, 1996.
- [22] J.J. Beaudoin, V.S. Ramachandran, R.F. Feldman, Interaction of chloride and C-S-H, *Cem Concr Res* 20 (1990) 875–883.
- [23] A.K. Suryavanshi, J.D. Scantlebury, S.B. Lyon, Mechanism of Friedel’s salt formation in cements rich in tri-calcium aluminate, *Cem Concr Res* 26 (1996) 717–727.
- [24] D.M. Roy, Mechanisms of cement paste degradation due to chemical and physical factors, Vol. I, Proceedings of the 8th International Congress on Chemistry of Cement, 362–380, Rio de Janeiro, 1986.
- [25] C.J. Pereira, L.L. Hegedus, Diffusion and reaction of chloride ions in porous concrete, in: Proceedings of the 8th International Symposium of Chemical Reaction Engineering, Edinburgh, 1984.
- [26] V.G. Papadakis, M.N. Fardis, C.G. Vayenas, Physicochemical processes and mathematical modeling of concrete chlorination, *Chem Eng Sci* 51 (1996) 505–513.
- [27] V.G. Papadakis, M.N. Fardis, C.G. Vayenas, Mathematical modeling of chloride effect on concrete durability and protection measures, in: R.K. Dhir, M.R. Jones (Eds.), *Concrete Repair, Rehabilitation and Protection*, E. & F.N. Spon, London, 1996, 165–174.
- [28] V.G. Papadakis, H. Lindgreen, E.J. Pedersen, An AFM-SEM investigation of the effect of silica fume and fly ash on cement paste microstructure, *J Mater Sci* 34 (1999) 683–690.
- [29] V.T. Ngala, C.L. Page, Effects of carbonation on pore structure and diffusional properties of hydrated cement pastes, *Cem Concr Res* 27 (1997) 995–1007.
- [30] S.W. Yu, C.L. Page, Diffusion in cementitious materials: I. Comparative study of chloride and oxygen diffusion in hydrated cement pastes, *Cem Concr Res* 21 (1991) 581–588.
- [31] C.M. Hansson, Oxygen diffusion through Portland cement mortars, *Corrosion Science* 35 (1993) 1551–1556.
- [32] R.K. Dhir, M.A.K. El-Mohr, T.D. Dyer, Developing chloride resisting concrete using PFA, *Cem Concr Res* 27 (1997) 1633–1639.